Review of Mold Flux Entrainment Mechanisms and Model Investigation of Entrainment by Shear-Layer Instability

Lance C. Hibbeler, Rui Liu and Brian G. Thomas
lhibbel2@illinois.edu, ruiliu1@illinois.edu, bgthomas@illinois.edu

The University of Illinois at Urbana-Champaign
Department of Mechanical Science and Engineering
1206 West Green Street, MC 244
Urbana, Illinois 61802
The United States of America

Abstract

This paper first presents a comprehensive review of flux entrainment in continuous casting molds, which is a major difficulty in the production of clean steel. By understanding the mechanisms that cause entrainment, the operating conditions of casters can be selected to find windows of safe operation that reduce the number of inclusion defects in the final steel product. Nine mechanisms have been proposed over the last three decades, including vortex formation around the submerged entry nozzle (SEN), argon bubble interactions with the slag layer such as "foaming," shear-layer or Kelvin-Helmholtz instability at the slag-steel interface, excessive upward flow impingement upon the meniscus at the narrow faces, top surface level fluctuations, meniscus freezing and hook formation, top surface "balding," top surface standing wave instability, and slag crawling down the SEN. The previous work to study each of these mechanisms is presented, including a qualitative description of the behavior, and any available quantitative criteria to predict their occurrence. Finally, the shear-layer instability mechanism is explored in detail, using transient numerical models of the turbulent-multiphase fluid flow phenomena in both oil-and-water and slag-and-steel systems. The slag-and-steel simulations include the effects of the temperature gradient in the slag layer and the temperature dependence of the slag viscosity. The numerical models are validated with an idealized analytical solution, and are also compared with previous experimental measurements that explored the mechanism. Finally, the critical meniscus velocity to avoid entrainment is presented and discussed.

Key words: Mold flux entrainment; inclusions; clean steel production; numerical model

Introduction

Mold flux/slag entrainment, also called emulsification, entrapment, involvement, or engulfment is an important problem in the production of clean steel. By any name, this phenomenon of interest in this work is characterized by droplets of melted mold powder being drawn into the molten steel pool inside a continuous casting mold. Mold flux entrainment can cause both surface and internal defects if the entrained particles become trapped in the solidifying steel. All of the previous work on this subject, regardless of the analysis method or entrainment mechanism, agrees that mold flux entrainment depends mainly on the physical properties of the materials involved (especially the density, viscosity, and interfacial tension of the steel and slag); the slag layer thickness; and the flow system design and operating conditions (especially nozzle geometry, casting speed, and argon gas flow rate).

Flux entrainment has received much attention over the years and several mechanisms have been proposed, which are summarized in this work. Many studies have used room-temperature physical models, usually with water and a silicon oil. Physical models are unable to match all of the relevant similarity criteria simultaneously, however, so their results are difficult to interpret quantitatively. The ever-advancing computer technology has also allowed numerical investigations of flux entrainment, although challenges related to turbulent and multiphase flow still remain. The computational models referred to in this paper usually treat turbulence with the k-ε model, though other models find occasional use.

Previous reviews of work on this topic include those of Herbertson *et al.* [1], Suzuki *et al.* [2], and Thomas [3], but a comprehensive picture of the mechanisms of mold flux entrainment remains elusive. Early work focused mainly on fluctuations of the meniscus level, which correlate strongly with defects. The entrainment mechanisms reported in later literature fall into eight more families: meniscus freezing, argon bubble interaction, slag "crawling" down the submerged entry nozzle (SEN), vortexing, top surface standing wave instability, shear-layer instability, narrow face spout impingement upon the meniscus, and meniscus balding. Most mechanisms suggest a critical condition for entrainment, which can be used to evaluate physical or numerical models of fluid flow in a caster. Entrainment is not detrimental to product quality unless the inclusions ultimately become caught in the

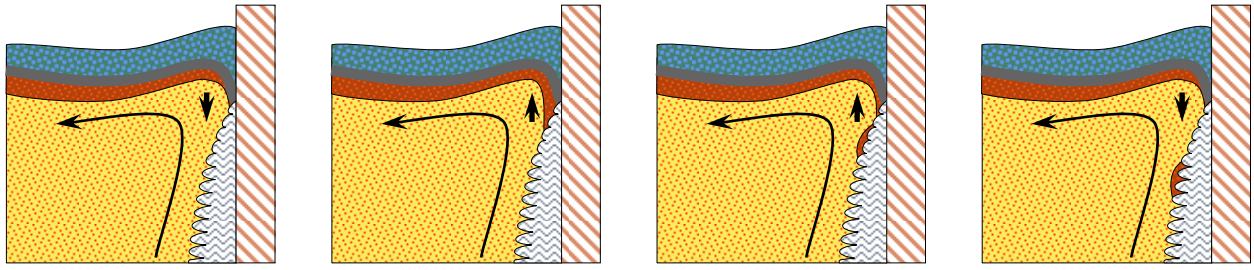

a) Start of Level Fluctuation | b) Slag-Shell Contact | c) Slag Trapped in Denrdites | d) End of Level Fluctuation

Figure 1: Entrainment by Meniscus Level Fluctuation

solidifying steel. Particles may or may not become entrapped in an approaching dendritic solidification front depending on the particle diameter, local cross-flow velocity, and steel composition [4]. Downward flow velocities may exacerbate entrapment by suspending the rising particles in front of the solidifying interface [5], which may explain why single-roll patterns are found to produce more slag entrapment defects [6]. The capacity of the liquid slag layer to absorb the inclusions that reach it depends greatly on the composition, and associated properties [7]. Dynamic models have been constructed for solid [8] and liquid [9] particles to determine if a particle will be absorbed into the slag layer, which decreases with decreasing inclusion particle diameter, decreasing wettability between the slag and particles, increasing interfacial tension, and increasing slag viscosity. However, these same properties which discourage inclusion removal often help to prevent entrainment from occurring at all.

The first part of this paper presents a critical overview of the nine families of mechanisms that cause entrainment of mold slag during continuous casting. The review adopts the following symbols: V is velocity, g is acceleration due to gravity, μ is molecular viscosity, ρ is density, and Γ_{AB} is interfacial tension between fluids A and B. The subscript u refers to the *upper* fluid layer (melted mold powder) and the subscript ℓ refers to the *lower* fluid layer (molten steel). SEN port angles are defined to increase when pointing less steeply downwards.

Meniscus Level Fluctuations

Many early studies on slag entrainment mechanisms focused on transient fluctuations of the meniscus, because they are observable and measurable in the steel plant. However, recent numerical models [10,11] showed how level fluctuations can entrain slag by exposing the dendritic interface of the top of the solidifying steel shell to liquid slag and mold powder during a sudden drop in the level. Fig. 1 shows the sequence of events leading to entrainment by this mechanism. Although oscillation causes slight changes in liquid level during each cycle, transient changes in the flow pattern in the mold are responsible for the large level fluctuations that cause severe slag entrainment defects.

Physical model studies have shown that meniscus fluctuations increase with increasing casting speed [12,13], increasing SEN bore diameter [14], increasing (*i.e.* more upwards) SEN port angles [12,14], decreasing SEN immersion depth [12], decreasing slab width [12], and increasing argon flow rate [12,14,15]. Poor wettability between the argon and SEN refractory increases the effect of argon on fluctuations [15], but increasing the casting speed decreases the effect of argon bubbles [12]. Single-roll flow patterns are more susceptible to defects via this mechanism, and combinations of flow-control variables that produce continuously unstable complex flow patterns are worst [16]. Electromagnetic forces offer another variable to control the flow pattern. Plant experiments using static (braking) or moving electromagnetic fields have reported decreases in level fluctuations and associated defects (*cf.* the review in the paper by Cukierski and Thomas [17]).

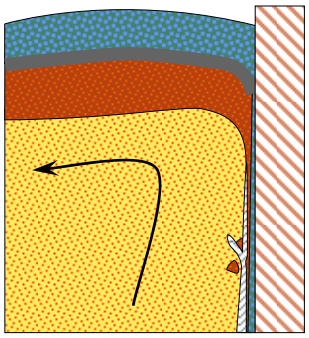

Figure 2: Hook Trapping A Particle

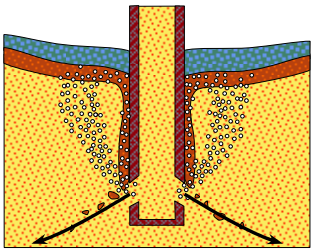

Figure 3: Slag Foaming

Meniscus Freezing and Hook Formation

Another mechanism for the entrainment of slag and inclusion particles to form surface defects is illustrated in Fig. 2, which shows a slag particle entrapped by a hook. The root cause of hook formation [18,19] is freezing of the meniscus, due to insufficient heat delivered to the meniscus region near the narrow face. The frozen meniscus may extend into the melt and capture rising bubbles or particles. In addition, overflowing of the frozen meniscus can entrap any slag coating its surface. Hooks can be prevented by

increasing flow velocity, increasing superheat, or increasing SEN port angles more upwards, all of which increase the heat supply to this region.

Flow conditions such as caused by a shallow SEN may produce excessive meniscus surface velocities which increase surface turbulence, leading to instability, entrapment, and uneven powder distribution, as discussed in the previous section. However, too deep an SEN can result in meniscus freezing, hook formation, and shell thinning below mold exit [20]. Kubota [13] demonstrated that electromagnetic forces may be used to increase flow velocities at lower casting speeds to avoid hook formation, and gave the condition that surface velocities should be kept above a lower limit of 0.15-0.25 m/s to minimize surface defects for the mold considered in the study.

Argon Bubble Interactions

Argon gas is usually fed into the SEN to help prevent nozzle clogging, which leads to problems from both nonmetallic inclusions and asymmetric fluid flow. Argon bubbles also add a buoyancy force to the steel flow that changes the flow pattern. Thus, argon injection may lessen some problems, such as hook formation, but is detrimental to other entrapment mechanisms, such as surface level fluctuations.

Emling *et al.* [21] found slab defects caused by argon gas bubbles coated with mold slag. They noted in a water model study that argon bubbles flowing out of the SEN can form a foam with the slag layer, which can adhere to and crawl down the outside of the nozzle and become caught in the nozzle jet, as shown in Fig. 3. The occurrence of the foam was found to increase with increasing slab width, increasing argon injection rate, increasing slag viscosity, decreasing slag density, and decreasing interfacial tension between the slag and steel [21]. Staying below a critical maximum argon flow rate was observed to reduce defects [21], and this critical value was later reported [15] to vary with casting speed, and increase with increasing slag layer viscosity, increasing wettability between the SEN refractory and molten slag, and steeper downward nozzle port angles.

Slag Crawling

A solid object submerged into a flowing liquid will result in a pressure buildup on the windward (right) side and a pressure drop in the leeward (left) side, as illustrated in Fig. 4a. When a free surface is present, these pressure changes will change the elevation of the surface. Asymmetric flow in a continuous casting mold can cause this situation to occur. This low-pressure zone might draw some liquid slag down along the outside of the SEN, and if severe enough, the slag might become entrained into the steel jet and be carried away to form defects, as shown in Fig. 4b.

Physical model experiments of flow past a circular cylinder [22] were performed to investigate this mechanism. The penetration depth h_p that the upper fluid crawls down the cylinder is:

$$h_p = 1.9 \frac{C_{p,max}\rho_u V_u^2 + C_{p,min}\rho_\ell V_\ell^2}{g(\rho_\ell - \rho_u)} \quad (1)$$

where $C_{p,max}$ = 1.0 and $C_{p,min}$ = 2.5 are the pressure coefficients for a circular nozzle. For elliptical nozzles, the coefficients to decrease with increasing aspect ratio a according to [23]:

$$C_{p,max} = 1.376 - 0.0652 \cdot a \quad (2)$$

$$C_{p,min} = 1.978 - 1.065 \cdot \ln(a) \quad (3)$$

where the aspect ratio is the ratio of the major diameter (parallel to the flow direction) to the minor diameter, so increasing the SEN aspect ratio lowers the penetration depth. To avoid entrainment by this mechanism, the SEN immersion depth should be greater than the slag penetration depth. Note that slag crawling and the slag foaming mechanism discussed previously can act together to aggravate entrainment [21], but this is not reflected in Eq. 1.

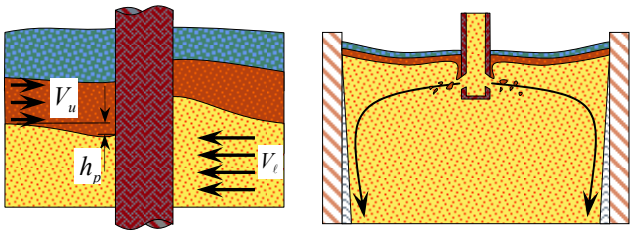

a) Slag Crawling Model *b) Slag Crawling w/ Shallow SEN*

Figure 4: Slag Crawling

von Kármán Vortex Formation

Flow past bluff bodies can result in the periodic shedding of vortices in the wake of the object. Asymmetric flow between sides of the mold is the source of flow through the narrow gap between the SEN and mold walls that causes vortices that entrain slag, as shown in Fig. 5. The slightest asymmetry can result in the formation of vortices, but this does not guarantee the entrainment of slag.

These vortices can entrain slag that becomes entrapped between the dendrites on the wide face near the SEN, leading to a sharp increase in the number of sliver defects in the center of the slabs [20]. Alternatively, vortices may pull a funnel of slag deep enough into the mold that the jet coming out of the SEN entrains the tip of the vortex, transporting slag-related inclusions elsewhere in the slab [24,25,26]. The vortices are always observed to form on the weaker side of the flow, *i.e.* in the wake of the SEN

[24,25,26,27,28,29,30]. Vortex depth increases with increasing meniscus surface velocity [24,28]. Vortex diameter increases with increasing casting speed [24] and SEN misalignment [24,25]. Vortex formation frequency increases with increasing slab width [20,29], shallower SEN immersion depths [20,26,29], increasing (less downward) SEN port angle [25,26], increasing casting speed [20,24,25,26,28], and increasing SEN misalignment [24,25].

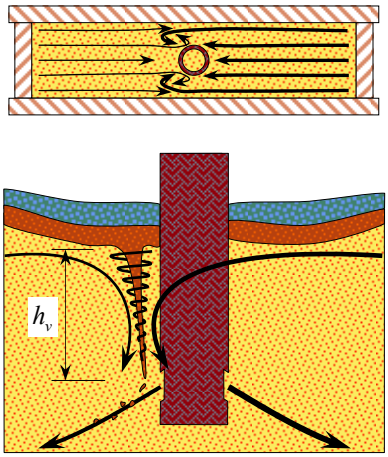

Figure 5: Vortexing Entrainment

Vortex formation needs both rotational flow in the plane of the meniscus, and a downward-pulling sink. The sink momentum is found where the opposing roll flows meet near the center of the mold [27,28]. A maximum velocity for vortex formation was also observed, because excessive velocities cause the meniscus to become too oscillatory and turbulent to allow the formation of vortices [26,28]. Computational models confirm that vortex formation cannot occur with perfectly symmetric geometry and flow conditions [24,31]. Meeting a critical meniscus velocity or flow rate criterion does not guarantee vortex formation [29], and furthermore, the presence of a vortex does not imply that slag will be entrained into the melt [26].

Increasing argon flow rates to above 10% gas fraction induces buoyancy that can decrease the downward velocity near the SEN and prevent vortex formation, but this reinforces asymmetric flow [24] and can also trigger the argon-related mechanisms discussed above. Vortex formation was reported to be suppressed with sufficiently strong electromagnetic braking to control the asymmetry of the flow [24,30]. Recent water modeling [26] has proposed a critical surface velocity for vortex formation of 0.3 m/s, as well as a prediction of vortex depth h_v:

$$h_v = \frac{V_{mc}^2}{g}\frac{\rho_\ell}{\rho_\ell - \rho_u} + c\left(\frac{\Delta V_s^2}{g}\frac{\rho_u}{\rho_\ell - \rho_u}\right)^{0.55} \qquad (4)$$

where V_{mc} is the horizontal steel velocity (m/s) in the center of the mold, 10 mm below the water-oil interface and halfway between the SEN and wide face, ΔV_s is the sudden change in vertical velocity, measured 50 mm below the steel-slag interface, 10 mm away from the SEN and halfway between the wide faces, and $C = 0.0562\,\mathrm{m}^{0.45}$ is a constant with all other quantities in m-kg-s units. This model predicts the SEN immersion depth needed to avoid the jets cutting of the tips of the vortices.

Meniscus Standing Wave Instability

Flow beneath a free liquid surface will create surface waves which can become unstable and turn over to entrain the interface, if the local slope becomes sufficiently steep (exceeding vertical) [32]. The flow in continuous casting molds leads to a stationary wave in the surface shape, excluding the local level fluctuations discussed previously. A stability criterion was proposed as a height-to-wavelength ratio [32,33]:

$$\left(h_{wave}/\lambda\right)_{crit} = 0.21 + 0.14\left(\rho_u/\rho_\ell\right)^2 \qquad (5)$$

where h_{wave} is the wave height defined as the vertical distance between the lowest point (trough) and highest point (crest) of the surface level and λ is the wavelength, defined as the distance between the outer SEN wall and the narrow faces [33,34,35]. Early experiments indicated this model is an overprediction and that a vortex forms at the node at lower height-to-wavelength ratios, indicating that the stability of the wave is governed by shearing at the interface, rather than by the wave turning over [32].

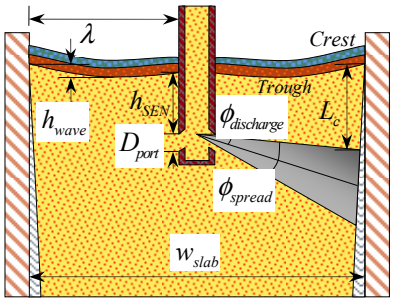

Figure 6: Standing Wave Instability

Eq. 5 can be used with any of the models available in the literature [29,33,34,36,37] that predict the wave height to create a criterion for critical SEN port velocity. For example, the wave height h_{wave} may be calculated as [33]:

$$h_{wave} = 0.31\frac{V_{port}^2}{g}\frac{D_{port}}{L_c}\frac{\rho_\ell + \rho_u}{\rho_\ell - \rho_u} \qquad (6)$$

where D_{port} is the diameter of the SEN ports, V_{port} is the velocity of the molten steel at the SEN ports, and

L_c is a characteristic length taken as the height of the upper recirculation zone, calculated as $L_c = h_{SEN} + \frac{1}{2} w_{slab} \tan\left(\phi_{discharge} - \frac{1}{2}\phi_{jet}\right)$ for immersion depth h_{SEN}, slab width w_{slab}, jet discharge angle $\phi_{discharge}$, and jet spread angle ϕ_{spread}, as shown in Fig. 6.

With a proper surface tension model, the wave instability event was successfully simulated numerically [38]. This numerical model showed a recirculating packet of fluid at the trough that disappeared after entrainment. This suggests that shear stresses form a horizontal vortex that causes the instability of the interface, which is a different mechanism, discussed in the next section. The highest surface velocities coincide with the trough of the standing wave [35,38,39], which again indicate that shear instability is the real cause of entrainment. None of the models in the literature investigated a steel-slag system, asymmetry effects, or combined effects of buoyancy, surface tension, and three-dimensional flow features. However, it appears likely that the standing wave height instability (turnover) mechanism is not a problem in practice, because shear instability occurs more easily.

Shear Layer Instability

The interface between two density-stratified fluids with relative motion will become unstable with a large-enough difference in velocity. A theoretical condition for this instability was derived by Helmholtz [40] and Kelvin [41] for two idealized fluids separated by a flat interface. Most researchers have identified shear instability of the interface to be a cause for mold slag entrainment, shown in Fig. 7, though little has been done to explore this mechanism. This fundamental hydrodynamic phenomenon of Kelvin-Helmholtz instability (KHI) has received considerable treatment over the last 150 years and is found throughout nature, including ocean waves and clouds. The interface between the fluids becomes unstable if the velocity difference between the two layers is greater than:

$$\Delta V_{crit} = \sqrt[4]{4g\left(\rho_\ell - \rho_u\right)\Gamma_{u\ell}\left[\rho_u^{-1} + \rho_\ell^{-1}\right]^2} \qquad (6)$$

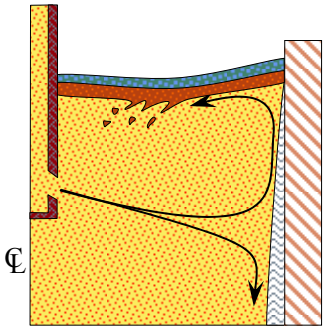

Figure 7: Shear Instability

Magnetic fields applied transverse to the flow direction do not affect the stability of the interface, and fields applied parallel to the flow direction have the same effect as surface tension in stabilizing the interface [42]. The physical model experiments of Iguchi *et al.* [43] confirmed the Milne-Thomson [44] extension of the Kelvin-Helmholtz theory to finite-depth fluids using low-viscosity oils, when surface tension is not important. This shear instability mechanism is most likely to occur midway between the narrow face and SEN where horizontal surface velocity is a maximum.

Upward Flow Impinging on Meniscus

The upward spout along the narrow faces resulting from a double-roll flow pattern may cause slag entrainment in both cutting [21] and dragging [45] and modes, illustrated in Figs. 8 and 9. This is an example of shear-layer instability where the geometric aspects of the flow render the Kelvin-Helmholtz theory inapplicable. Harman and Cramb [45] developed the following relation, based on measurements of oil-and-water model experiments:

$$V_{crit} = 3.065 \frac{\Gamma_{u\ell}^{0.292}\, g^{0.115}}{\delta^{0.365}} \frac{\left(\rho_\ell - \rho_u\right)^{0.215}}{\rho_u^{0.694}} \frac{\mu_u^{0.231}}{\mu_\ell^{0.043}} \qquad (7)$$

Entrainment occurs more easily with lower water (steel) density, lower interfacial tension, lower oil (slag) viscosity, and increasing slag layer thickness δ. This work was repeated [46] for a wider property range and more controlled flow patterns and resulted in similar trends, except for the effect of slag layer thickness.

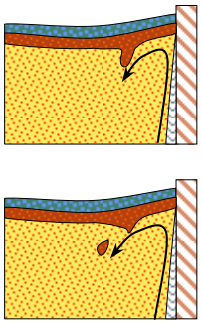

Figure 8: NF Spout, Dragging Mode

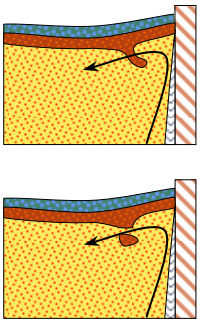

Figure 9: NF Spout, Cutting Mode

Top Surface Balding

In a worst-case scenario, some of the above mechanisms for slag entrainment can push the slag layer out of the way, as shown in Figs. 10 and 11. This phenomenon is named “balding” of the top surface, as it exposes molten steel to the sintered and solid powder layers of the slag layer, if not the atmosphere. This can occur in continuous casting at high nozzle flow rates [39], and the accompanying surface re-oxidation forms inclusions such as alumina. Also, particles of powder can become entrained at the bald spot, especially if it coincides with the trough of

the standing wave [39]. Meniscus balding may be prevented by having a slag layer thickness at least the size of the standing wave height [37], such as predicted from Eq. 6. Excessive argon flow rates [47] can also cause balding, as illustrated in Fig. 14.

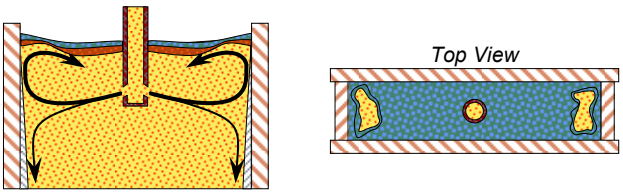

Figure 10: Balding by Excessive NF Spout

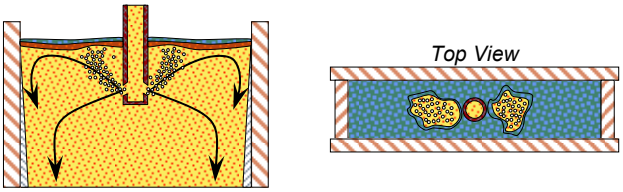

Figure 11: Balding by Excessive Argon Flow

Discussion

Designing and operating a caster to avoid entrainment requires careful selection of many different inter-related parameters, to find a window of stable, entrainment-free operation. Casting conditions must be found to simultaneously avoid each of the above mechanisms. The various equations presented here can be used together as design tools or to help evaluate the results of a numerical or physical model of flow in the caster. In using these equations, it should be noted that critical conditions for a given mechanism are often exceeded due to asymmetric flow conditions, even though symmetric time-averaged conditions would have safely avoided entrainment.

There is no single optimum solution. For example, the choice of slag layer properties should balance the conflicting needs to use the slag as an inclusion catcher (which requires low interfacial tension) with preventing shear instability (which requires high interfacial tension). Further work is needed to include chemical composition and mass transfer effects at the interface [7], which can significantly change the interfacial tensions.

Entrainment by vortex formation combined with related exacerbating mechanisms is likely the most common mechanism of entrainment, owing to the ease at which asymmetric flow can occur. The stability of the standing wave, the impinging narrow face spout, and bone fide Kelvin-Helmholtz instability are all different embodiments of the same mechanism: parallel shear-layer instability. Preventing shear instability requires control of surface velocity. Maintaining a safe surface velocity requires selection of SEN parameters and electromagnetic forces to avoid large meniscus fluctuations and shear instability, while keeping the meniscus temperatures warm enough to prevent hook formation.

Modeling Study

A modeling study has been performed to further investigate the shear-layer instability mechanism of entrainment halfway between the SEN and NF mold. The theoretical Kelvin-Helmholtz instability (KHI) model provides an analytical criterion that was used to verify the numerical model used in this study. Consider an *inviscid* molten steel-slag system with ρ_u = 3500 kg/m³, ρ_ℓ = 7000 kg/m³, and $\Gamma_{u\ell}$ = 1.1 N/m. The two-dimensional modeling domain for this verification problem was a 0.2×0.4-m rectangle with periodic boundary conditions on the vertical edges and fixed velocities on the horizontal edges. The volume of fluid (VOF) model was used to treat the multiple phases present in the problem, with the continuum surface force (CSF) model treating surface tension effects. The domain was initialized with the lower fluid at a prescribed velocity, which was varied as part of the verification effort, and the upper fluid was initialized at rest. The interface between the two fluids was perturbed sinusoidally with amplitude of one cell height and a frequency that varied as part of the verification effort. The prescribed horizontal wall velocities matched these initial velocities. The model was integrated forward in time with the PISO (pressure-implicit with splitting of operators) scheme, and the results were analyzed for stability. The results are given in Fig. 12, along with the predictions of Eq. 6.

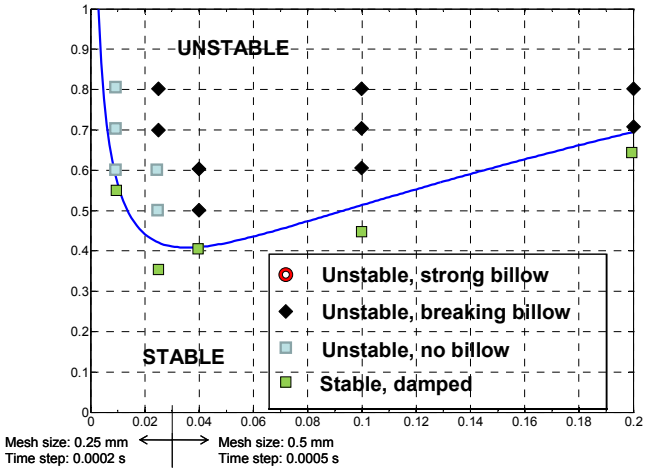

Figure 12: Verification Problem Results

The analytical KHI model predictions are binary: either the interface is stable or it is not. The numerical simulations showed degrees of instability, judged by whether or not the characteristic Kelvin-Helmholtz billows were predicted to form in the simulation and how violently the fluids mixed, as described in Fig. 13. With proper interpretation, the numerical model is able to match the analytical predictions of the conditions for an unstable interface.

The analytical KHI criterion is far too removed from the conditions found in a continuous caster to be of any practical use, and so the numerical model was next adapted to include a finite slag layer thickness of 10 mm, a linear temperature gradient through the slag layer (causing 650 ºC difference), and temperature-dependent viscosity in both fluids, as calculated in previous work [48]. Fig. 14 shows the temperature-dependent viscosity profile and Fig. 15 shows the viscosity as a function of position through the slag layer.

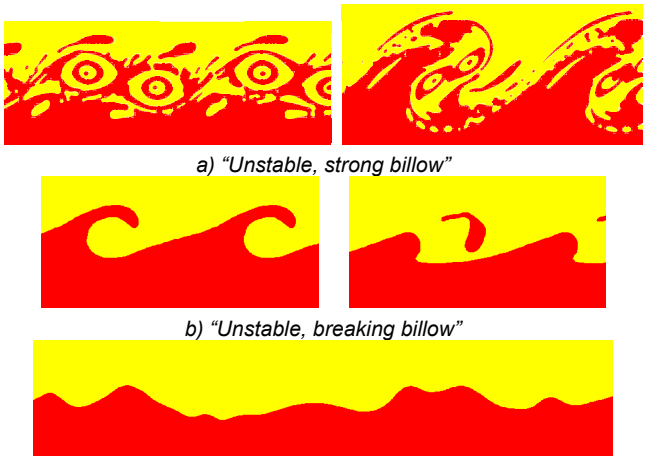

a) "Unstable, strong billow"

b) "Unstable, breaking billow"

c) "Unstable, no billow"

Figure 13: Unstable Interface Descriptions

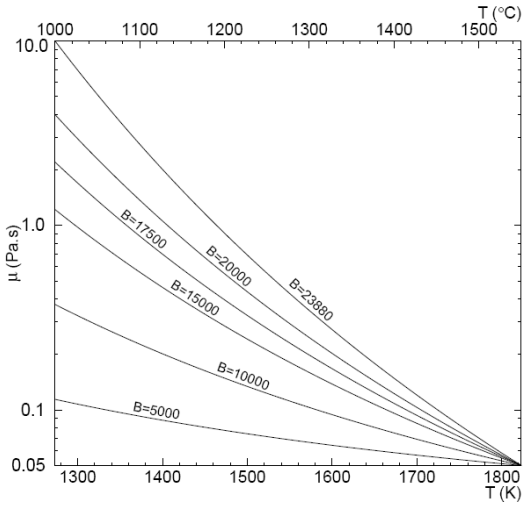

Figure 14: Temperature-Dependent Viscosity of Slag

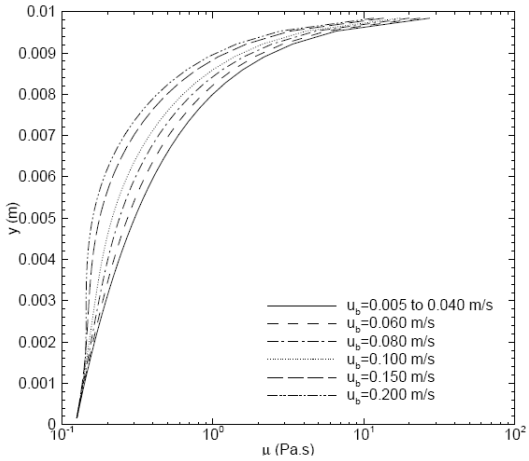

Figure 15: Viscosity as a Function of Position in Slag

The modeling domain for this case was set up very similar to the verification problem, only with a finite domain length of 0.1 m with prescribed inlet velocities on the left side and pressure outlets on the right side. The interface perturbation frequencies were taken as 25 mm and 25 mm with 30 mm superimposed. The significance of 25 mm is that it is the capillary wavelength, the wavelength at which surface tension and gravitational effects precisely balance and when the analytical KHI criterion takes on its minimum. The idea of superimposing wavelengths is to simulate the randomness of turbulent flow found in casters.

The velocity differences investigated were 0.7, 0.9, 1.0, and 1.1 m/s. The interfaces in the first three cases are described as "unstable, no billow" and in fact returned to a stable, quiescent interface because of the viscous effects tending to dampen out the drive to instability caused by the parallel-flowing shear layer. The interface in the case of 1.1 m/s velocity difference across is described as "unstable, strong billow," with clear evidence of the occurrence of flux entrainment, *i.e.*, particles of molten slag drawn into and carried away in the molten steel flow, as illustrated in Fig. 16.

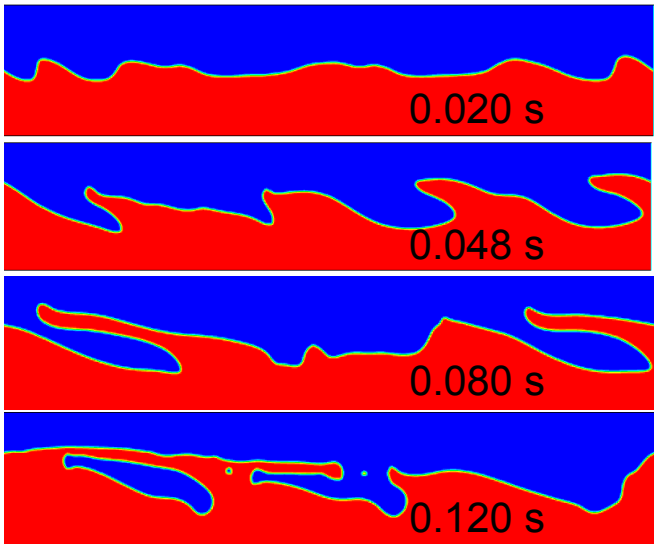

Figure 16: Simulated Mold Flux Entrainment by KHI

Note, however, that the interface velocity necessary to cause entrainment, rather than just instability, is 1.1 m/s. This value is much higher than the 0.3-0.4 m/s that is generally observed in casters. This does not imply, however, that this mechanism of entrainment can never occur. Velocities on the order of this have been observed in water models that encounter asymmetric flow through uneven SEN port discharge [49]. Furthermore, the surface tension can be drastically reduced in the presence of a chemical reaction at the interface, reducing the critical surface velocity to ranges that are readily achievable in casters with normal flow conditions.

Conclusions

Many studies have been performed over the years to investigate mold slag entrainment, which is one of the main sources of inclusion defects in continuous casting of steel. This work identifies nine distinct mechanisms responsible for entrainment, especially vortexing due to asymmetric flow, argon bubble interactions with the slag layer, shear-layer instability at the slag-steel interface, and excessive upward flow impingement on the meniscus. Other important mechanisms include meniscus level fluctuations, meniscus freezing and hook formation, and meniscus balding. Standing wave instability appears unlikely as shear-layer instability can occur more easily. The slag layer can also crawl down the SEN, which is important at shallow submergence depths or with slag foaming. The various simple models available in previous literature to roughly quantify these nine mechanisms are summarized here, and can be used to help evaluate the results of computational models of the flow field in the molten steel pool. Predictions are further complicated, however, because the different mechanisms can act together to aggravate entrainment. Much future work is needed to develop better prediction tools for this important problem.

The modeling study to investigate the shear-layer instability mechanism was able to successfully match the analytical Kelvin-Helmholtz model predictions of an unstable interface, and identified that there are varying degrees of the concept “unstable” depending on the magnitude of the velocity jump across the interface. The model was extended to include the effects of typical viscosity and temperature gradients through the slag layer and found that a surface velocity of 1.1 m/s was needed to cause slag entrainment for an interfacial tension of 1.1N/m. Hence, the apparent effect of viscosity is to stabilize the interface and prevent slag entrainment. Although this result tends to show that this entrainment mechanism is not likely during normal casting, the critical surface velocity may be exceeded during conditions of asymmetric flow, or property changes such as a lower interfacial tension.

Acknowledgements

The authors gratefully acknowledge the financial support of the member companies of the Continuous Casting Consortium at the University of Illinois.

References

[1] Herbertson, J.; He, Q.L.; Flint, P.J.; Mahapatra, R.B.: Modelling of Metals Delivery to Continuous Casting Moulds; 74th Steelmaking Conf. Proc., 1991, P. 171-185

[2] Suzuki, M.; Suzuki, M; Nakada, M.: Perspectives of Research on High-Speed Conventional Slab Continuous Casting of Carbon Steels; ISIJ Int., 41 (2001), No. 7, P. 670-682

[3] Thomas, B.G.: Modeling of Continuous-Casting Defects Related to Mold Fluid Flow; Proc. 3rd Int. Cong. Sci. Tech. Steelmaking, 2005, P. 847-861

[4] Yuan Q.; Thomas, B.G.: Transport and Entrapment of Particles in Continuous Casting of Steel; Proc. 11th Modeling of Casting, Welding, Advanced Solidification Processes, 2006, P. 745-752

[5] Lee, G.-G.; Shin, H.-J.; Thomas, B.G.; Kim, S.-H.: Asymmetric Multi-Phase Fluid Flow and Particle Entrapment in a Continuous Casting Mold; Proc. AISTech 2008, P. 63-73

[6] Kunstreich, S.; Dauby, P.H.: Effect of Liquid Steel Flow Pattern on Slab Quality and the Need for Dynamic Electromagnetic Control in the Mould; Ironmaking Steelmaking, 32 (2005), No. 1, P. 80-86

[7] Cramb, A.W.; Chung, Y.; Harman, J.; Sharan, A.; Jimbo, I.: The Slag/Metal Interface and Associated Phenomena; Iron Steelmaker, 24 (1997), No. 3, P. 77-83

[8] Bouris, D.; Bergeles, G.: Investigation of Inclusion Re-Entrainment from the Steel-Slag Interface; Metall. Met. Trans. B, 29 (1998), No. 3, P. 641-649

[9] Strandh, J; Nakajima, K.; Eriksson, R.; Jönsson, P.: A Mathematical Model to Study Liquid Inclusion Behavior at the Steel-Slag Interface; ISIJ Int., 45 (2005), No. 12, P. 1838-1847

[10] Ojeda, C; Thomas, B.G.; Barco, J.; Arana, J.L.; Model of Thermal-Fluid Flow in the Meniscus Region During an Oscillation Cycle; Proc. AISTech 2007, P. 269-283

[11] Sengupta, J.; Ojeda, C.; Thomas, B. G.: Thermal-Mechanical Behaviour during Initial Solidification in Continuous Casting: Steel Grade Effects; Int. J. Cast Metals Res., 22 (2009), No. 1-4, P. 8-14

[12] Teshima, T.; Osame, M.; Okimoto, K.; Nimura, Y.: Improvement of Surface Property of Steel at High Casting Speed; 71st Steelmaking Conf. Proc., 1988, P. 111-118

[13] Kubota, J.; Okimoto, K.; Shirayama, A.; Murakami, H.; Meniscus Flow Control in the Mold by Travelling Magnetic Field for High Speed Slab

Caster; 74th Steelmaking Conf. Proc., 1988, P. 233-241
[14] Nakato, H.; Saito, K.; Oguchi, Y.; *et al.*: Surface Quality Improvement of Continuously Cast Blooms by Optimizing Solidification in Early Stage; 70th Steelmaking Conf. Proc., 1987, P. 427-431
[15] Wang, Z.; Mukai, K.; Ma, Z.; *et al.*: Influence of Injected Ar Gas on the Involvement of the Mold Powder Under Different Wettabilities Between Porous Refractory and Molten Steel; ISIJ Int., 39 (1999), No. 8, P. 795-803
[16] Kunstreich, S.; Dauby, P.H.; Baek, S.-K.; Lee, S.-M.: Multi-Mode EMS in thick slab casters molds and effect on coil quality and machine performance; 5th European Continuous Casting Conf., 2005, S14_12 P037
[17] Cukierski, K.; Thomas, B.G.: Flow Control with Local Electromagnetic Braking in Continuous Casting of Steel Slabs; Metall. Met. Trans. B, 39 (2008), No. 1, P. 94-107
[18] Sengupta, J.; Thomas, B.G.; Shin, H.-J.; *et al.*: A New Mechanism of Hook Formation during Continuous Casting of Ultra-Low-Carbon Steel Slabs; Metall. Met. Trans. A, 37 (2006), No. 5, P. 1597-1611
[19] Lee, G.-G.; Thomas, B.G.; Kim, S.-H.; *et al.*: Microstructure Near Corners of Continuous-Cast Steel Slabs Showing Three-Dimensional Frozen Meniscus at Hooks; Acta Mat., 55 (2007), No. 20, P. 6705-6712
[20] Wang, Y.H.: A Study of the Effect of Casting Conditions on Fluid Flow in the Mold Using Water Modelling; 73rd Steelmaking Conf. Proc., 1990, P. 473-480
[21] Emling, W.H.; Waugaman, T.A.: *et al.*, "Subsurface Mold Slag Entrainment in Ultra Low Carbon Steels; 77th Steelmaking Conf. Proc., 1994, P. 371-379
[22] Yoshida, J.; Ohmi, T.; Iguchi, M.: Cold Model Study on the Effects of Density Difference and Blockage Factor on Mold Powder Entrainment; ISIJ Int., 45 (2005), No. 8, P. 1160-1164
[23] Ueda, Y.; Kida, T.; Iguchi, M.: Unsteady Pressure Coefficient Around an Elliptic Immersion Nozzle; ISIJ Int., 44 (2004), No. 8, P. 1403-1409
[24] Li, B.; Okane, T.; Umeda, T.: Modeling of Biased Flow Phenomena Associated with the Effects of Static Magnetic-Field Application and Argon Gas Injection in Slab Continuous Casting of Steel; Metall. Met. Trans. B, 32 (2001) No. 6, P. 1053-1066
[25] Li. B.; Tsukihashi, F.: Vortexing Flow Patterns in a Water Model of Slab Continuous Casting Mold; ISIJ Int., 45 (2005), No. 8, P. 30-36
[26] Kasai, N; Iguchi, M.: Water-Model Experiment on Melting Powder Trapping by Vortex in the Continuous Casting Mold; ISIJ Int., 47 (2007), No. 7, P. 982-987
[27] He, Q.: Observations of Vortex Formation in the Mould of a Continuous Slab Caster; ISIJ Int., 33 (1993), No. 2, P. 343-345
[28] Gebhard, M.; He, Q.L.; Herbertson, J.: Vortexing Phenomena in Continuous Slab Casting Moulds; 76th Steelmaking Conf. Proc., 1993, P. 441-446
[29] Gupta, D.; Lahiri, A.K.: Water-Modeling Study of the Surface Disturbances in Continuous Slab Caster; Metall. Met. Trans. B, 25 (1994), No. 2, P. 227-233
[30] Li, B.; Tsukihashi, F.: Effects of Electromagnetic Brake on Vortex Flows in This Slab Continuous Casting Mold; ISIJ Int., 46 (2006), No. 12, P. 1833-1838
[31] Kastner, G.; Brandstätter, W.; Kaufmann, B.; *et al.*: Numerical Study on Mould Powder Entrapment Caused by Vortexing in a Continuous Casting Process; Steel Res. Int., 77 (2006), No. 6, P. 404-408
[32] Rottman, J.W.: Steep Standing Waves at a Fluid Interface; J. Fluid Mech., 124 (1982), P. 283-306
[33] Theodorakakos, A.; Bergeles, G.: Numerical Investigation of the Interface in a Continuous Steel Casting Mold Water Model; Metall. Met. Trans. B, 29 (1998), No. 6, P. 1321-1327
[34] Panaras, G.A.; Theodorakakos, A.; Bergeles, G.: Numerical Investigation of the Free Surface in a Continuous Steel Casting Mold; Metall. Met. Trans. B, 29 (1998), No. 5, P. 1117-1126
[35] Anagnostopoulos, J.; Bergeles, G.: Three-Dimensional Modeling of the Flow and the Interface Surface in a Continuous Casting Mold Model; Metall. Met. Trans. B, 30 (1999), No. 6, P. 1095-1105
[36] Moghaddam, B.S.; Steinmetz, E.; Scheller, P. R.; Interaction Between the Flow Condition and the Meniscus Disturbance in the Continuous Slab Caster; Proc. 3rd Int. Cong. Sci. Tech. Steelmaking, 2005, P. 911-920
[37] Gupta, D.; Lahiri, A.K.: Cold Model Study of the Surface Profile in a Continuous Slab Casting Mold: Effect of Second Phase; Metall. Met. Trans. B, 27 (1996), No. 4, P. 695-697
[38] Dash, S.K.; Mondal, S.S.; Ajmani, S.K.: Mathematical Simulation of Surface Wave Created in a Mold Due to Submerged Entry Nozzle; Int. J. Num. Meth. Heat Fluid Flow, 14 (2004), No. 5, P. 606-632
[39] Gupta, D.; Lahiri, A.K.: Cold Model Study of Slag Entrainment into Liquid Steel in Continuous Slab Caster; Ironmaking Steelmaking, 23 (1996), No. 4, P. 361-363
[40] von Helmholtz, H.L.F.: Über discontinuierliche Flueßigkeits-Bewegungen; Monatsb. K. Preuss. Akad. Wiss. Berlin, 23 (1868), P. 215-228
[41] Thomson, W. (Lord Kelvin): Hydrokinetic Solutions and Observations; Phil. Mag., 42 (1871), No. 281, P. 362-377

[42] Cha, P.; Yoon, J.: The Effect of a Uniform Direct Current Magnetic Field on the Stability of a Stratified Liquid Flux/Molten Steel System; Metall. Met. Trans. B, 31 (2000), No. 2, P. 317-326
[43] Iguchi, M.; Yoshida, J.; Shimizu, T.; Mizuno, Y.: Model Study on the Entrapment of Mold Powder into Molten Steel; ISIJ Int., 40 (2000), No. 7, P. 685-691.
[44] Milne-Thomson, L.M.: *Theoretical Hydrodynamics*, 5e. Macmillan Press, London, (1968).
[45] Harman, J.M.; Cramb, A.W.: A Study of the Effect of Fluid Physical Properties upon Droplet Emulsification; Proc. 79th Steelmaking Conf., 1996, P. 773-784
[46] Savolainen, J.; Fabritius, T.; Mattila, O.: Effect of Fluid Physical Properties on the Emulsification; ISIJ Int., 49 (2009), No. 1, P. 29-36
[47] Harris, D.J.; Young, J.D.: Water Modeling – A Viable Production Tool; Proc. 65th Steelmaking Conf., 1982, P. 3-16
[48] Zhao, B.; Vanka, S.P.; Thomas, B.G.: Numerical Study of Flow and Heat Transfer in a Molten Flux Layer; Int. J. Heat Fluid Flow, 26 (2005), No. 1, P. 105-118
[49] He, Q.; Evans, G.; Serje, R.; Jaques, T.: Fluid Flow and Mold Slag Entrainment in the Continuous Twin-Slab Casting Mould; Proc. AISTech 2009, P. 573-588